

## Article

# Methods for Constructing a Refined Early-Warning Model for Rainstorm-Induced Waterlogging in Historic and Cultural Districts

Jing Wu <sup>1</sup>, Junqi Li <sup>1,2,\*</sup>, Xiufang Wang <sup>3</sup>, Lei Xu <sup>4</sup>, Yuanqing Li <sup>1</sup>, Jing Li <sup>1</sup>, Yao Zhang <sup>5</sup> and Tianchen Xie <sup>5</sup> 

- <sup>1</sup> Key Laboratory of Urban Stormwater System and Water Environment, Ministry of Education, Beijing University of Civil Engineering and Architecture, Beijing 100044, China; wujing0625@126.com (J.W.)
- <sup>2</sup> Beijing Energy Conservation & Sustainable Urban and Rural Development Provincial and Ministry Co-Construction Collaboration Innovation Center, Beijing 100044, China
- <sup>3</sup> School of Science, Beijing University of Civil Engineering and Architecture, Beijing 102616, China
- <sup>4</sup> The Institute of Archaeology & College of Applied Arts and Science, Beijing Union University, Beijing 100191, China
- <sup>5</sup> Engineering Research Center of Engineering Structures and New Materials & School of Civil and Transportation Engineering, Beijing University of Civil Engineering and Architecture, Beijing 100044, China
- \* Correspondence: lijunqi@bucea.edu.cn

**Abstract:** Against the backdrop of increasingly severe global climate change, the risk of rainstorm-induced waterlogging has become the primary threat to the safety of historic and cultural districts worldwide. This paper focuses on the historic and cultural districts of Beijing, China, and explores techniques and methods for identifying extreme rainstorm warnings in cultural heritage areas. Refined warning and forecasting have become important non-engineering measures to enhance these districts' waterlogging prevention control and emergency management capabilities. This paper constructs a rainstorm-induced waterlogging risk warning model tailored for Beijing's historical and cultural districts. This model system encompasses three sets of models: a building waterlogging early-warning model, a road waterlogging early-warning model, and a public evacuation early-warning model. During the construction of the model, the core concepts and determination methods of "1 h rainfall intensity water logging index" and "the waterlogging risk index in historical and cultural districts" were proposed. The construction and application of the three models take into full account the correlation between rainfall intensity and rainwater accumulation, while incorporating the characteristics of flood resilience in buildings, roads, and the society in districts. This allows for a precise grading of warning levels, leading to the formulation of corresponding warning response measures. Empirical tests have shown that the construction method proposed in this paper is reliable. The innovative results not only provide a new perspective and method for the early-warning of rainstorm-induced waterlogging, but also offer scientific support for emergency planning and response in historical and cultural districts.

**Keywords:** early-warning model; rainstorm; waterlogging; cultural heritage sites; historic and cultural districts; emergency management; flood resilience



**Citation:** Wu, J.; Li, J.; Wang, X.; Xu, L.; Li, Y.; Li, J.; Zhang, Y.; Xie, T. Methods for Constructing a Refined Early-Warning Model for Rainstorm-Induced Waterlogging in Historic and Cultural Districts. *Water* **2024**, *16*, 1290. <https://doi.org/10.3390/w16091290>

Academic Editor: Maria Mimikou

Received: 25 March 2024

Revised: 21 April 2024

Accepted: 29 April 2024

Published: 30 April 2024



**Copyright:** © 2024 by the authors. Licensee MDPI, Basel, Switzerland. This article is an open access article distributed under the terms and conditions of the Creative Commons Attribution (CC BY) license (<https://creativecommons.org/licenses/by/4.0/>).

## 1. Introduction

Historic and cultural districts are areas with rich cultural relics, concentrated historic buildings, and the ability to reflect traditional patterns and historic features in a relatively intact and authentic manner at a certain scale. In the context of global climate change, extreme rainfall events are becoming increasingly frequent, and rainstorm disasters and urban waterlogging have become the primary risk threatening the safety of historic and cultural districts [1–3]. According to incomplete statistics, in just one year, 2021, there were 223 such events that occurred worldwide, far exceeding the number of rainstorm disasters in the past decade. Flood disasters in historic and cultural districts can be classified into

seven types: breaches, overflow, waterlogging, flood routing and storage, flash floods, storm surges, and tsunamis. Waterlogging disaster refers to a disaster caused by excessive or continuous precipitation that exceeds the urban drainage capacity, resulting in the accumulation of water within the city that cannot be drained in a timely manner. Cultural heritage sites located in plain areas are mostly concentrated in the old urban areas of historic and cultural districts, characterized by a long history, dense population, high development intensity, low-lying land, and poor regional drainage, making them highly susceptible to widespread water accumulation and subsequent internal waterlogging risks [4]. These risks may cause irreversible local damage or destruction to cultural heritage sites. Once the tangible cultural heritage is damaged, it is difficult to restore, and the losses in terms of historic, cultural, and economic value resulting from rainstorm-induced waterlogging are incalculable. Urban waterlogging has become a serious threat to the security of historic and cultural heritage sites worldwide [5].

In the past two decades, research and practices in international disaster management have gradually shifted toward proactive disaster risk management, moving away from traditional passive response approaches [6]. Regarding strategy selection, there is an increasing emphasis on integrating structural and non-structural measures to overcome the limitations of excessive reliance on structural measures and neglect of non-structural measures [7]. In terms of governance models, there has been a shift from the traditional top-down approach dominated by historic urban management to a more flexible and grassroots-oriented governance mechanism for historic and cultural districts [8]. This evolution not only reflects the gradual maturation of the theoretical framework of disaster management theory, but also provides crucial insights for enhancing the effectiveness of emergency control and management against waterlogging in historical and cultural districts [9].

Considering the severity of the current situation, waterlogging prevention control has become a critical and urgent task. In particular, under the constraints of spatial control systems in historic and cultural districts, non-engineering measures such as refined warning systems will play a crucial role [10]. Accurate early-warning systems serve as a vital tool, providing indispensable objective insights into potential disaster-prone regions for effective emergency preparedness and response [11]. Furthermore, they play a pivotal role in ensuring the seamless and safe execution of rescue and emergency operations within historical and cultural districts, thus safeguarding their integrity and safety. Therefore, research and practices in refined warning systems for rainstorm-induced waterlogging should be highly valuable [12]. Scientific methods and technological means should be employed to enhance the accuracy and timeliness of warnings, providing strong decision-making support for waterlogging prevention control efforts in historic and cultural districts [13].

Certain research achievements have accumulated in the field of rainstorm-induced waterlogging risk warning [14]. These studies mainly focus on constructing models and consider core elements such as meteorological rainfall warnings [15,16], warning indicators [17,18], waterlogging depths [19], warning thresholds [20,21], and emergency plans [22], demonstrating a certain level of practicality. However, when such early-warning models are applied to small-scale areas such as historic and cultural districts, issues arise, including imprecise guidance and underestimated risk assessments. The root causes of the issues can be primarily attributed to the following four aspects: Firstly, the assessment methods of early-warning models possess limitations. Some research outcomes rely on indicator system approaches to evaluate flood risk levels [23]. However, this method struggles to accurately capture the specific flood risk differences among various hazard-affected bodies within urban districts, such as buildings, roads, and the public. Consequently, the classification of warning levels tends to be overly general and even underestimates the actual risks. Therefore, independent assessments and warning systems tailored for critical hazard-affected bodies like buildings, roads, and the public are imperative to enhance the precision and effectiveness of early warnings. Secondly, the determination methods for the relationship between meteorological forecasts and urban waterlogging responses

require further optimization. Current monitoring-reliant warning technologies are subject to uncertainties and lags, which undermine the accuracy and timeliness of early warnings [24]. Hence, there is a need to explore warning methods that are independent of monitoring data. Thirdly, the evaluation of waterlogging risks for different hazard-affected bodies within districts, including buildings, roads, and the public, remains inadequate. Compared to traditional risk assessment methods, flood resilience evaluation offers a more effective reflection of the actual risks posed by rainstorm-induced waterlogging [25–28]. Therefore, it is crucial to strengthen the assessment and research on the flood resilience of various hazard-affected bodies to provide a scientific basis for developing more targeted waterlogging prevention and emergency response measures [29,30]. Lastly, the issue of bridging the gap between early-warning results and emergency responses is frequently overlooked. Given the pre-judgment of warning levels, there is an urgent need to formulate both technical and non-technical emergency response measures. Consequently, it is essential to strengthen the linkage between early warnings and emergency responses to ensure prompt and effective implementation of appropriate emergency measures following the issuance of warnings, thereby minimizing disaster losses.

Based on the above research requirements, the objectives of this paper are as follows: (1) To propose a method for constructing a fine-grained model for early warning of rainstorm-induced waterlogging in historical and cultural districts, aiming to establish three sets of fine-grained models, including the building waterlogging early-warning model, road waterlogging early-warning model, and public evacuation early-warning model; (2) To introduce the concept of 1 h rainfall intensity water logging index, aiming to explore a reliable method for determining the response relationship between rainfall intensity and rainwater accumulation based on model simulation and clustering algorithms without relying on monitoring data; (3) To put forward the concepts of building waterlogging risk index, road waterlogging risk index, and public evacuation index, aiming to determine the values of the three indices by assessing the flood resilience of buildings, roads, and communities in the blocks; and (4) To develop early-warning response measures for building waterlogging, road waterlogging, and public evacuation in Beijing's historical and cultural districts based on the four-level warning grades for buildings, roads, and the public. The research results of this paper not only contribute to improving the accuracy and timeliness of early warnings, but also effectively address the issue of how to strengthen the linkage between early warning, emergency management, and meteorological forecasting work. This will provide more scientific decision support for the preparation of emergency response plans and pre-disaster emergency preparations in historical and cultural districts, providing different levels of warning information for waterlogging control work, thereby guiding the efficient implementation of emergency rescue and evacuation efforts.

## 2. Materials and Methods

### 2.1. Study Area

The research work of this paper was conducted in the historical and cultural districts of Beijing, China. These districts hold unique heritage value and are an indispensable part of Beijing's protection system for its historic and cultural heritage. They embody the historical memory and cultural essence of Beijing, playing a crucial role in bridging the past with the future, preserving traditions, and promoting innovation. Over the past three decades, Beijing has actively delineated and protected its historic and cultural districts, establishing 49 such districts by the end of 2021. These regions, located in the urban area of Beijing, experience a temperate monsoon climate with distinct seasons, hot summers with abundant rainfall, and a relatively high frequency of localized heavy rainstorms. Local climatic conditions can lead to short-duration, high-intensity, small-scale localized sudden rainstorms, which can easily cause localized waterlogging. Therefore, selecting Beijing's historic and cultural districts as the research focus offers a highly representative case and provides valuable insights into the practical application of refined early-warning models for rainstorm-induced waterlogging across diverse urban areas.

## 2.2. Construction Method of a Refined Early-Warning Model for Rainstorm-Induced Waterlogging in the Historic and Cultural Districts of Beijing

The refined early-warning model for rainstorm-induced waterlogging in Beijing's historic and cultural districts is composed of three core modules: the building waterlogging early-warning model, the road waterlogging early-warning model, and the public evacuation early-warning model, as detailed in Figure 1, outlining the technical approach to model construction. These three sets of models address the diverse warning needs for buildings, roads, and public evacuations by thoroughly analyzing and characterizing the complex response relationships among building waterlogging risk, road waterlogging risk, and public evacuation and rainfall intensity forecasts. Through the simulation of hydrological and hydrodynamic models, the correlation between rainfall intensity and the depth of surface water accumulation in the district is revealed. Currently, models applied to flood simulation both domestically and internationally include SWMM, HEC-RAS, PCSWMM, MIKE, InfoWorks ICM, etc. After establishing the model network, high-precision DEM raster data of the study area, as well as vector data of building layers, road layers, river layers, waterway layers, and greenbelt layers, are imported into the model in sequence [31,32]. Given that the surface runoff time in Beijing's historic and cultural districts is generally less than 1 h, in this study, 2 h short-duration design rainfall data with return periods of 100 years, 200 years, 500 years, and 1000 years were selected as the input parameters for simulating rainstorm events. Based on this correlation, a key indicator, namely, 1 h rainfall intensity water logging index, was defined. By assessing the flood resilience of disaster-bearing bodies within the historical and cultural district, significant differences in waterlogging risk among various disaster-bearing bodies are revealed. The three critical indicators required in the model, namely, the building waterlogging risk index, the road waterlogging risk index, and the public evacuation index, are all negatively correlated with their corresponding flood resilience assessment levels. The three sets of early-warning models are logically interconnected and functionally complementary, collectively constructing the complete warning mechanism of the refined early-warning model for rainstorm-induced waterlogging in Beijing's historic and cultural districts. Detailed discussions will follow from the perspectives of index determination methods and model construction methods.

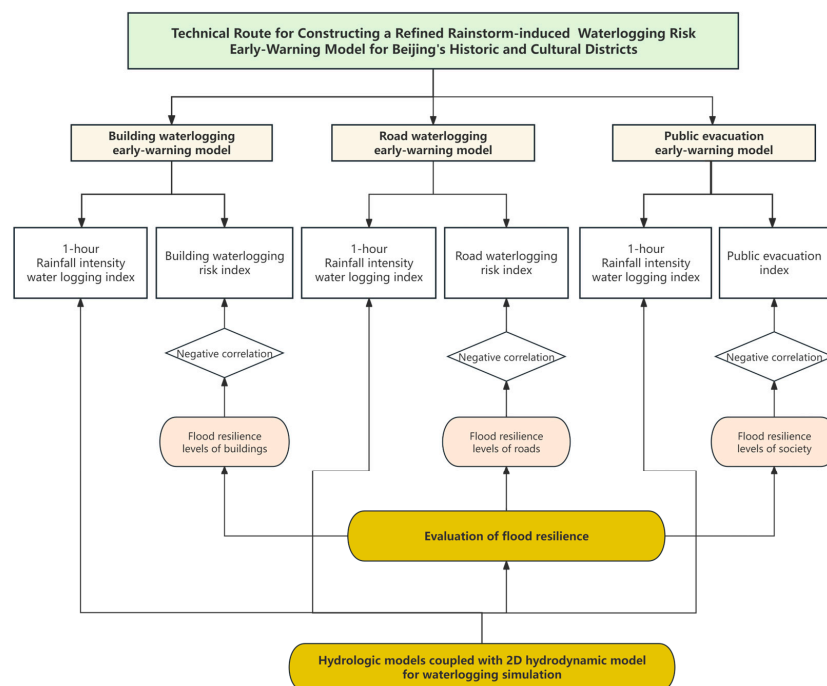


**Figure 1.** Technical route for constructing a refined rainstorm-induced waterlogging risk early warning model for Beijing's historic and cultural districts.

### 2.2.1. Determination Method for the 1 h Rainfall Intensity Water Logging Index in Beijing's Historic and Cultural Districts

The 1 h rainfall intensity serves as a frequently utilized parameter in meteorological forecasts. Linking the hourly rainfall intensity with the characteristics of rainstorm-induced waterlogging in the district can effectively inform warning efforts for rainstorm-induced waterlogging risk in Beijing's historic and cultural districts. Hence, this paper introduces the concept and determination method of the 1 h rainfall intensity water logging index. Utilizing the unsupervised learning algorithm of K-Means clustering, a quantitative assessment of the response relationship between 1 h rainfall intensity and regional water accumulation in the area was conducted. It should be noted that the  $x_R$  value is released by the meteorological department. During early warning, the 1 h rainfall intensity is known data, and its prediction method and related theories are beyond the scope of this paper.

The segmentation function of 1 h rainfall intensity water logging index  $f(x_R)$  in historic and cultural districts is shown in formula (1), where

$$f(x_R) = \begin{cases} 1, & x_R < x_{R1} \\ 2, & x_{R1} \leq x_R < x_{R2} \\ 3, & x_R \geq x_{R2} \end{cases} \quad (1)$$

where  $f(x_R)$  is 1 h rainfall intensity water logging index;  $x_R$  is the forecasted value of the 1 h rainfall intensity by the meteorological department (mm/h);  $x_{R1}$  is the upper threshold of 1 h rainfall intensity corresponding to low risk of waterlogging (mm/h);  $x_{R2}$  is the upper threshold of 1 h rainfall intensity corresponding to moderate risk of waterlogging (mm/h).

### 2.2.2. Determination Method for the Waterlogging Risk Index in Beijing's Historic and Cultural Districts

The waterlogging risk index in historic and cultural districts comprises three indicators: the building waterlogging risk index, the road waterlogging risk index, and the public evacuation index. These indicators are used to quantitatively assess the resistance, absorption, adaptability, and recovery capabilities of buildings, roads, and the public in the districts during waterlogging risk, which are represented by piecewise functions, respectively.

In this paper, flood resilience refers to the comprehensive response capability demonstrated by historical and cultural districts when encountering rainstorm waterlogging disasters, including resistance, coping, absorption, adaptation, and recovery. The resilience indicators encompass multiple dimensions such as physical resilience, organizational resilience, social resilience, and economic resilience [33–37].

Based on the method for calculating flood resilience in historic and cultural districts, the mathematical relationships between the flood resilience of buildings, roads, and society and characteristic parameters such as waterlogging depth and flow velocity can be determined. After cluster analysis, resilience levels can be obtained. The segmented values of these resilience levels are variable and should be dynamically adjusted based on each district's actual resilience calculation results. The higher the flood resilience levels of buildings, roads, and society in a district are, the lower the corresponding waterlogging risk, thus revealing a negative correlation between flood resilience levels and waterlogging risk indices. This paper divides flood resilience into three levels, namely, high, medium, and low, corresponding to risk indices of 1, 2, and 3, respectively.

The segmentation functions for the building waterlogging risk index  $f(Res_{BD})$ , road waterlogging risk index  $f(Res_{RD})$ , and public evacuation index  $f(Res_{OC})$  are represented by Equations (2)–(4), respectively. These equations depict the potential risk levels that buildings, roads, and the public may face during rainstorm-induced waterlogging.

$$f(Res_{BD}) = \begin{cases} 1, & Res_{BD} \geq Res_{BD1} \\ 2, & Res_{BD2} \leq Res_{BD} < Res_{BD1} \\ 3, & Res_{BD} < Res_{BD2} \end{cases} \quad (2)$$

$$f(Res_{RD}) = \begin{cases} 1, & Res_{RD} \geq Res_{RD1} \\ 2, & Res_{RD2} \leq Res_{RD} < Res_{RD1} \\ 3, & Res_{RD} < Res_{RD2} \end{cases} \quad (3)$$

$$f(Res_{OC}) = \begin{cases} 1, & Res_{OC} \geq Res_{OC1} \\ 2, & Res_{OC2} \leq Res_{OC} < Res_{OC1} \\ 3, & Res_{OC} < Res_{OC2} \end{cases} \quad (4)$$

where  $f(Res_{BD})$  is the building waterlogging risk index;  $Res_{BD1}$  is the lower threshold value corresponding to high flood resilience of district buildings (dimensionless);  $Res_{BD2}$  is the lower threshold value corresponding to medium flood resilience of district buildings (dimensionless);  $f(Res_{RD})$  is the road waterlogging risk index;  $Res_{RD1}$  is the lower threshold value corresponding to high flood resilience of district roads (dimensionless);  $Res_{RD2}$  is the lower threshold value corresponding to medium flood resilience of district roads (dimensionless);  $f(Res_{OC})$  is the public evacuation index of the district;  $Res_{OC1}$  is the lower threshold value corresponding to the high flood resilience of the district society (dimensionless);  $Res_{OC2}$  is the lower threshold value corresponding to medium flood resilience of the district society (dimensionless).

### 2.2.3. Construction Method for a Waterlogging Early-Warning Model in Beijing’s Historic and Cultural Districts

To ensure consistency with the rainstorm warning level system issued by the meteorological department and district-level flood warning systems in Beijing, the waterlogging early-warning models for buildings, roads, and public evacuation in the district use a standardized four-level warning system, represented by blue, yellow, orange, and red colors. This standardized warning system not only improves the efficiency and accuracy of responding to rainstorms and waterlogging disasters but also helps emergency response departments, rescue personnel, and the general public understand and promptly respond to warning information. Using intuitive color coding allows for clear differentiation of potential emergency response needs for different buildings, roads, and evacuation areas, ensuring the prompt implementation of effective measures to safeguard people’s lives and property to the greatest extent possible.

The building waterlogging early-warning model is denoted as  $f(W_{BD})$ , the road waterlogging early-warning model is denoted as  $f(W_{RD})$ , and the public evacuation early-warning model is denoted as  $f(W_{OC})$ . These early-warning models comprehensively reflect the coupling relationships between hourly rainfall intensity and building waterlogging risk, road waterlogging risk, and public evacuation. Mathematically, they are expressed as the product of 1 h rainfall intensity water logging index and the building waterlogging risk index, road waterlogging risk index, and public evacuation index. The mathematical expressions for the function models are given by Equations (5)–(7).

$$f(W_{BD}) = f(x_R) \times f(Res_{BD}) = \begin{cases} \text{Blue Alert,} & W_{BD} = 1 \\ \text{Yellow Alert,} & W_{BD} = 2 \\ \text{Orange Alert,} & W_{BD} \in [3, 4] \\ \text{Red Alert,} & W_{BD} \in [6, 9] \end{cases} \quad (5)$$

$$f(W_{RD}) = f(x_R) \times f(Res_{RD}) = \begin{cases} \text{Blue Alert,} & W_{RD} = 1 \\ \text{Yellow Alert,} & W_{RD} = 2 \\ \text{Orange Alert,} & W_{RD} \in [3, 4] \\ \text{Red Alert,} & W_{RD} \in [6, 9] \end{cases} \quad (6)$$

$$f(W_{OC}) = f(x_R) \times f(Res_{OC}) = \begin{cases} \text{Blue Alert,} & W_{OC} = 1 \\ \text{Yellow Alert,} & W_{OC} = 2 \\ \text{Orange Alert,} & W_{OC} \in [3, 4] \\ \text{Red Alert,} & W_{OC} \in [6, 9] \end{cases} \quad (7)$$

where  $f(W_{BD})$  is the building waterlogging early-warning model for the district;  $f(W_{RD})$  is the road waterlogging early-warning model for the district;  $f(W_{OC})$  is the public evacuation early-warning model for the district;  $W_{BD}$  is the numerical value obtained from the product of 1 h rainfall intensity water logging index  $f(x_R)$  and the building waterlogging risk index  $f(Res_{BD})$ ;  $W_{RD}$  is the numerical value obtained from the product of 1 h rainfall intensity water logging index  $f(x_R)$  and the road waterlogging risk index  $f(Res_{RD})$ ;  $W_{OC}$  is the numerical value obtained from the product of 1 h rainfall intensity water logging index  $f(x_R)$  and the public evacuation index  $f(Res_{OC})$ .

### 3. Results and Discussion

In this paper, the InfoWorks ICM software(9.5.5.19020) was utilized to establish a simulation model for rainstorm-induced waterlogging in Beijing's historic and cultural districts [38,39]. Using the Beijing II region rainfall intensity calculation formula, a 120 min rainfall process was inferred, and the maximum rainfall in each period with a time step of 5 min was accurately distributed [40–42].

The model to be validated in this study is the overland flow model. Model validation was performed using actual rainfall data from 9 August 2020, with a rainfall time step of 5 min. The model's accuracy was assessed through a comparative analysis between the simulation results and the actual waterlogging locations, achieving an average likelihood of 84%. A total of five locations were evaluated. Specifically, at Location 1, the maximum simulated depth was 12 cm compared to the measured waterlogging depth of 15 cm, yielding a likelihood of 80%. For Location 2, the maximum simulated depth was 14 cm versus the measured depth of 15 cm, resulting in a likelihood of 93%. At Location 3, the maximum simulated depth was 28 cm compared to the actual depth of 32 cm, giving a likelihood of 88%. For Location 4, the maximum simulated depth was 16 cm while the measured depth was 20 cm, leading to a likelihood of 80%. Finally, at Location 5, the maximum simulated depth was 10 cm compared to the measured depth of 13 cm, which corresponded to a likelihood of 77%. The model demonstrated high simulation accuracy and good applicability and reliability through calibration and validation with actual rainfall data. This hydrologic and hydrodynamic model can provide simulated data on the waterlogging depth, velocity, and duration, which can be used for the determination of the 1 h rainfall intensity water logging index and the evaluation of flood resilience levels in historic and cultural districts. Figure 2 illustrates the simulated results of the maximum waterlogging depth and the distribution of waterlogging in a historic and cultural district in Beijing under four typical return periods.

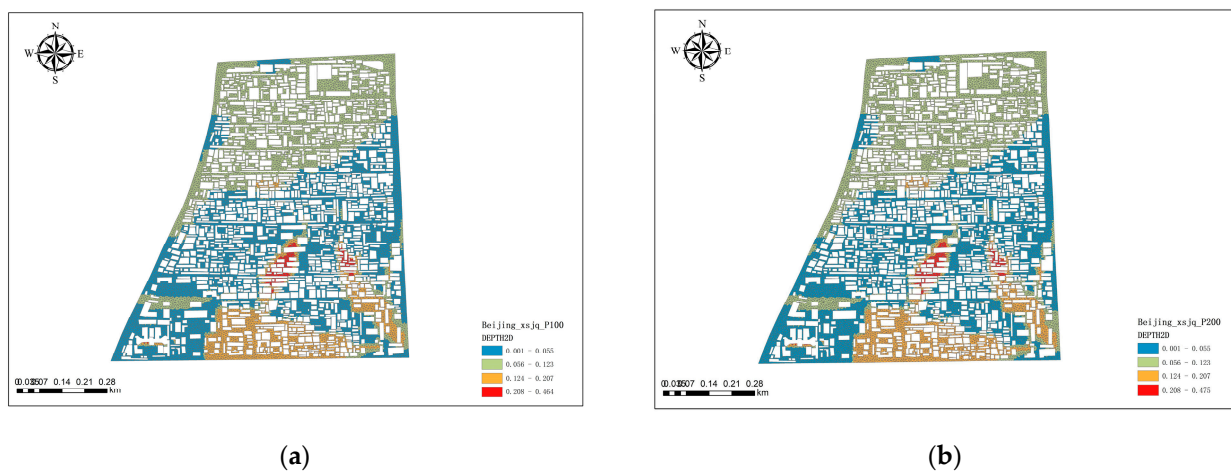
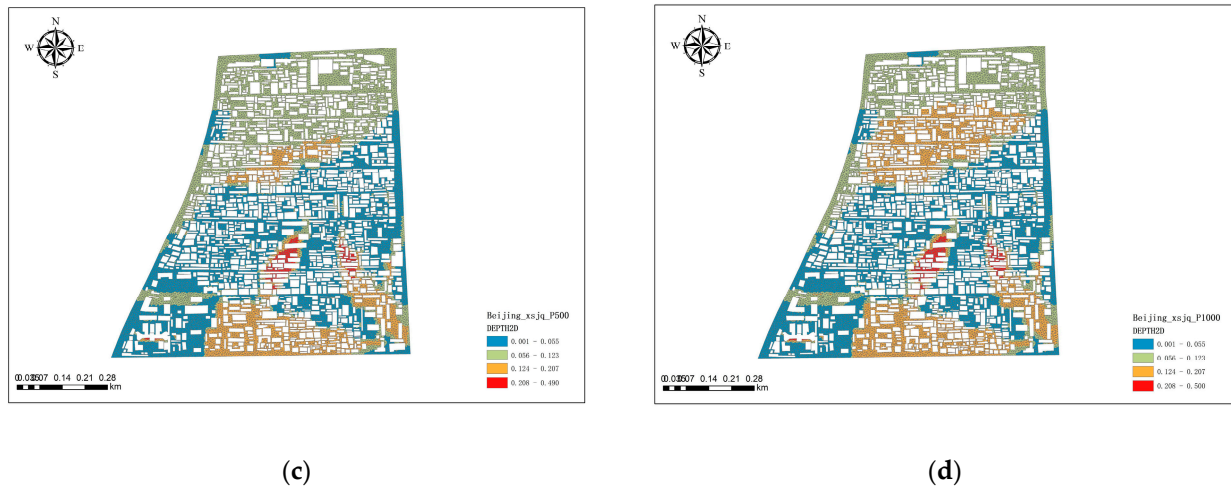


Figure 2. Cont.



**Figure 2.** Distribution map of simulated results for the maximum waterlogging depth in a historic and cultural district in Beijing under four typical return periods: (a) For the P100 scenario; (b) For the P200 scenario; (c) For the P500 scenario; and (d) For the P1000 scenario.

In Figure 2, the red areas represent high-risk zones, orange areas represent medium-high risk zones, green areas represent medium-risk zones, and blue areas represent low-risk zones. The main waterlogging areas in this block are located in the red and orange zones, primarily distributed in the central, southern, and northern regions of the block. The water accumulation in the central red high-risk zone is primarily attributed to the local topographical depression, where water from surrounding areas accumulates in the depression. A large orange medium-high-risk area appears in the southern region because water from the higher ground in the central region flows along the roads and converges in the orange low-lying areas, forming a large area of waterlogging. The cause of waterlogging in the northern region is due to the inflow of rainwater runoff from outside the block. A large amount of rainwater from outside the block flows into the block along the roads in the west. The depth and extent of waterlogging gradually increase with increasing rainfall intensity. This is reflected in the figure as the green medium-risk area gradually evolving into an orange medium-high-risk area, with the orange area appearing to be the largest in Figure 2d.

### 3.1. Determination of 1 h Rainfall Intensity Water Logging Index in Beijing's Historic and Cultural Districts

By utilizing the hydrologic and hydrodynamic model for simulation and adhering to the principle of worst-case scenario analysis, it is feasible to accurately pinpoint the most waterlogging-prone and critical locations within a designated historic and cultural district in Beijing. Furthermore, a detailed analysis is conducted to investigate the response relationship between the 1 h rainfall intensity and the depth of accumulated rainwater at the waterlogging-prone point under four typical return periods. The correlation between the two factors is identified, and based on this, 1 h rainfall intensity water logging index for a certain historic and cultural district is ultimately derived. As shown in Figure 3 below, the waterlogging-prone point begins to accumulate rainwater when the 1 h rainfall intensity exceeds 29.96 mm/h under the P100 scenario, exceeds 33.99 mm/h under the P200 scenario, exceeds 35.97 mm/h under the P500 scenario, and exceeds 40.00 mm/h under the P1000 scenario.

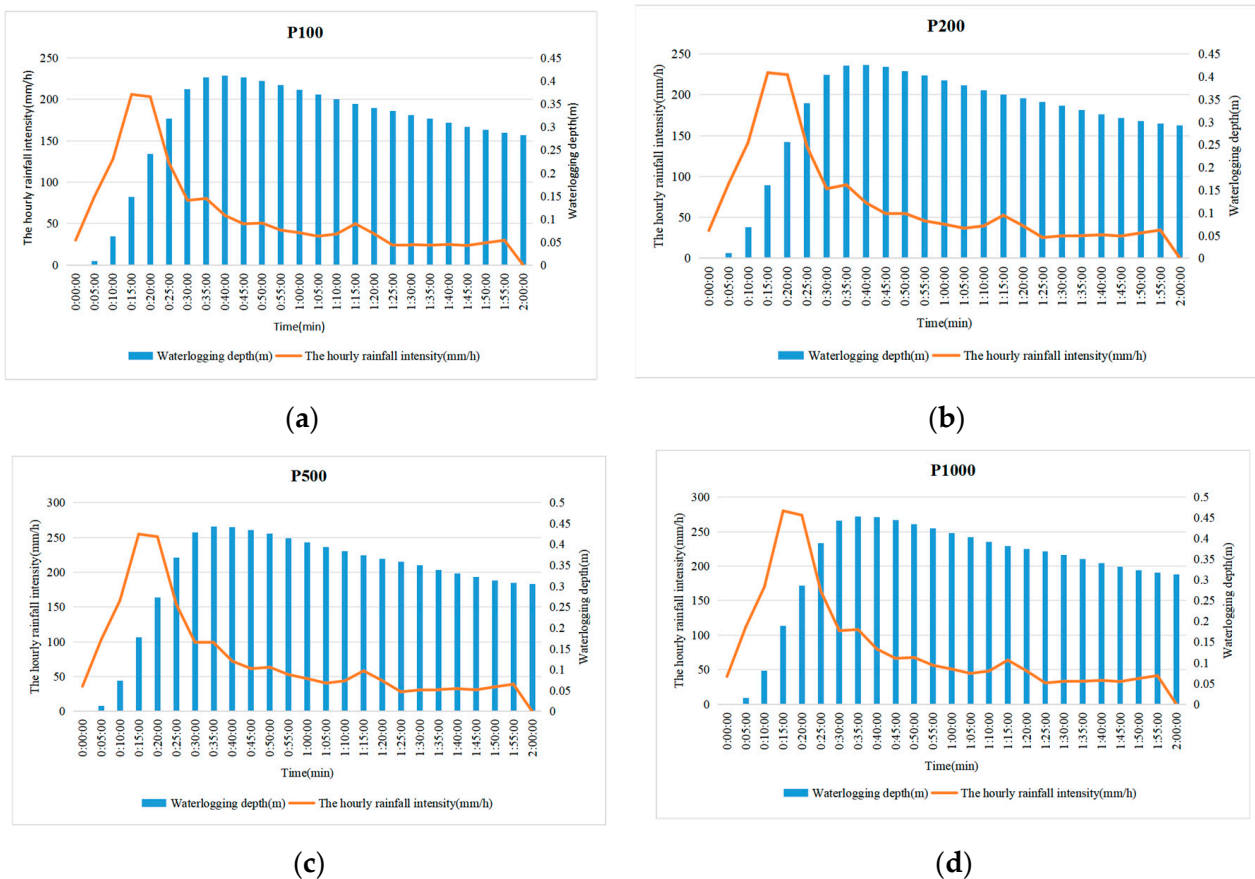


**Figure 3.** Response relationship between 1 h rainfall intensity and waterlogging depth at a certain waterlogging-prone point in Beijing’s historic and cultural districts under four typical return periods: (a) For the P100 scenario; (b) For the P200 scenario; (c) For the P500 scenario; (d) For the P1000 scenario.

To further quantify the clustering effect between 1 h rainfall intensity and district waterlogging, this paper utilized a centroid-based clustering algorithm (K-Means algorithm) to conduct a cluster analysis on the simulated model data of a specific waterlogging-prone point in the district under the four typical return periods, as depicted in Figure 2 above. As one of the classic clustering algorithms, the K-means algorithm has been widely applied in engineering fields and has significant advantages in handling datasets and discovering the inherent structure among data [43,44]. The Euclidean distance was chosen as the measure of similarity between data samples, where data samples within each cluster exhibited a certain degree of similarity in terms of both rainfall intensity and waterlogging depth. Through multiple iterations of calculation, the sum of the distances between each sample and the center of its respective cluster was minimized, ultimately dividing the sample data into eight categories. The analysis results are presented in Table 1 below. Among them, cluster 1 has a frequency of 42, accounting for 42.0% of the total; while cluster 5 has a frequency of 21, accounting for 21.0%. This indicates that clusters 1 and 5 exhibit strong data clustering effects. In contrast, the proportions of other clusters are relatively lower, with percentages below 11%.

Table 2 presents the outcomes of the differential analysis pertaining to the quantitative data fields obtained from the cluster analysis. The data include the mean value  $\pm$  standard deviation, F test results, and significant *p*-values. The significance *p*-value of the variable “rainfall intensity” (mm/h) is 0.000. The significance *p*-value of the variable “waterlogging depth” (m) is 0.003. Both variables exhibit significance at the specified level, rejecting the null hypothesis. This indicates that there are significant differences in “rainfall inten-

sity" (mm/h) and "waterlogging depth" (m) among the clusters identified through the clustering analysis.

**Table 1.** The clustering analysis results of the relationships between 1 h rainfall intensity and waterlogging depth at a specific waterlogging-prone points in a Beijing's historic and cultural districts under four typical return periods.

Index	Cluster Category	Frequency	Percentage%
1	Cluster 1	42	42.0
2	Cluster 2	6	6.0
3	Cluster 3	4	4.0
4	Cluster 4	11	11.0
5	Cluster 5	21	21.0
6	Cluster 6	4	4.0
7	Cluster 7	8	8.0
8	Cluster 8	4	4.0
Total		100	100

**Table 2.** Results of the clustering analysis of the quantitative field variability data.

	Cluster Category (Mean Value $\pm$ Standard Deviation)								F	p
	Cluster 1 (n = 42)	Cluster 5 (n = 21)	Cluster 4 (n = 11)	Cluster 7 (n = 8)	Cluster 2 (n = 6)	Cluster 6 (n = 4)	Cluster 8 (n = 4)	Cluster 3 (n = 4)		
Rainfall Intensity (mm/h)	32.852 $\pm$ 5.530	52.400 $\pm$ 6.269	78.228 $\pm$ 8.733	109.841 $\pm$ 10.828	154.425 $\pm$ 13.029	215.261 $\pm$ 12.265	0.000 $\pm$ 0.000	264.909 $\pm$ 14.200	895.328	0.000
Waterlogging Depth (m)	0.306 $\pm$ 0.104	0.398 $\pm$ 0.023	0.349 $\pm$ 0.169	0.272 $\pm$ 0.205	0.220 $\pm$ 0.161	0.202 $\pm$ 0.055	0.298 $\pm$ 0.014	0.232 $\pm$ 0.056	3.437	0.003

To validate the reliability of the clustering analysis results after multiple iterations, further calculations were conducted to evaluate the contour coefficient, DBI, and CH index. The higher the value of the contour coefficient index, the better the clustering effect. The smaller the value of the DBI metric, the better the clustering effect it represents. Similarly, a larger value of the CH indicates superior clustering performance. Through trial calculations with cluster numbers ranging from 3 to 9, it was determined that the comprehensive performance of all three metrics is optimal when the number of clusters is 8. As shown in Table 3, the clustering analysis exhibited excellent clustering performance. Using the K-means clustering algorithm to analyze the correlation between rainfall intensity and waterlogging depth demonstrates significant rationality and practicality, providing an analytical basis for determining the 1 h rainfall intensity water logging index.

**Table 3.** Evaluation metrics for clustering analysis.

Contour Coefficient	DBI	CH
0.592	0.432	895.137

To comprehensively determine the values of  $x_{R1}$  and  $x_{R2}$  in formula (1), it is necessary to further identify the response relationship between 1 h rainfall intensity of moderate to low intensity and waterlogging depth. Based on the clustering analysis results shown in Figure 4, Clusters 1 and 5 encompass data on moderate- and low-intensity 1 h rainfall, with numerical ranges between 23.57 and 63.79 mm/h. Consequently, this paper conducts an in-depth analysis of the data results for Clusters 1 and 5 to more precisely reveal the intrinsic link between rainfall of moderate to low intensity and waterlogging depth.

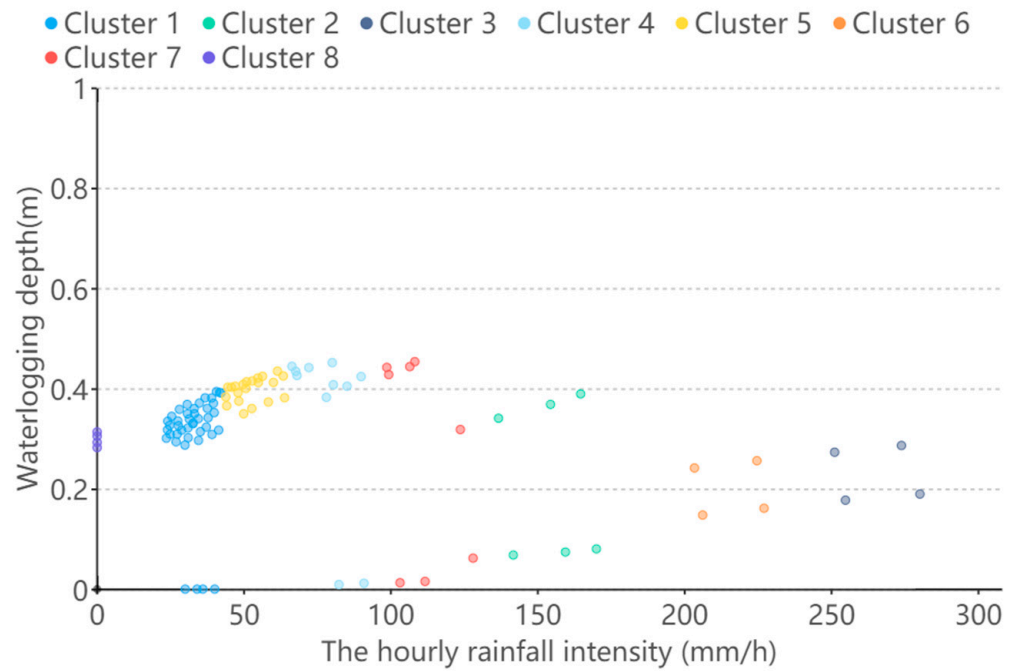


**Figure 4.** Scatter Plot of the clustering analysis for the response relationships between hourly rainfall intensity and waterlogging depth at a specific waterlogging point in Beijing’s historic and cultural districts under four typical return periods.

As shown in Table 4, Cluster 1 mainly groups the response data with 1 h rainfall intensity ranging from 23 to 42 mm/h and waterlogging depth ranging from 0 to 0.39 m. According to the principles of compiling urban waterlogging risk maps in Beijing, 0.27 m is the critical threshold between low and moderate risk of waterlogging. For the corresponding four sets of data in Table 4, where the waterlogging depth is 0, the range of 1 h rainfall intensity values corresponds to 30 and 40 mm/h. Therefore, 40 mm/h is selected as the corresponding 1 h rainfall intensity value  $x_{R1}$  for the critical threshold between low and medium risks. This value is consistent with the cumulative rainfall amount of 41 mm for a design rainfall intensity for a 2-year return period with a 1 h duration, which aligns with the current drainage capacity of Beijing’s historical and cultural districts.

**Table 4.** List of the response relationships between 1 h rainfall intensity and waterlogging depth in Cluster 1.

Index	Cluster Category	Rainfall Intensity (mm/h)	Waterlogging Depth (m)	Index	Cluster Category	Rainfall Intensity (mm/h)	Waterlogging Depth (m)
1	Cluster 1	40	0.39	22	Cluster 1	32	0.33
2	Cluster 1	41	0.39	23	Cluster 1	24	0.33
3	Cluster 1	42	0.39	24	Cluster 1	27	0.33
4	Cluster 1	36	0.38	25	Cluster 1	37	0.32
5	Cluster 1	38	0.38	26	Cluster 1	31	0.32
6	Cluster 1	34	0.37	27	Cluster 1	24	0.32
7	Cluster 1	39	0.37	28	Cluster 1	41	0.32
8	Cluster 1	30	0.37	29	Cluster 1	28	0.32
9	Cluster 1	37	0.36	30	Cluster 1	35	0.31
10	Cluster 1	33	0.36	31	Cluster 1	27	0.31
11	Cluster 1	28	0.36	32	Cluster 1	24	0.31
12	Cluster 1	39	0.35	33	Cluster 1	39	0.31

Table 4. Cont.

Index	Cluster Category	Rainfall Intensity (mm/h)	Waterlogging Depth (m)	Index	Cluster Category	Rainfall Intensity (mm/h)	Waterlogging Depth (m)
13	Cluster 1	33	0.35	34	Cluster 1	31	0.30
14	Cluster 1	30	0.35	35	Cluster 1	23	0.30
15	Cluster 1	25	0.35	36	Cluster 1	34	0.30
16	Cluster 1	37	0.35	37	Cluster 1	26	0.29
17	Cluster 1	34	0.34	38	Cluster 1	30	0.29
18	Cluster 1	31	0.34	39	Cluster 1	30	0
19	Cluster 1	27	0.33	40	Cluster 1	33	0
20	Cluster 1	24	0.33	41	Cluster 1	36	0
21	Cluster 1	32	0.33	42	Cluster 1	40	0

Table 5 demonstrates that Cluster 5 primarily encompasses response data characterized by 1 h rainfall intensities ranging from 43 to 63 mm/h and waterlogging depths varying between 0.35 and 0.43 m. Pursuant to the guidelines for compiling Beijing’s urban waterlogging risk maps, 0.40 m establishes the demarcation between moderate and higher risks of waterlogging. In alignment with this principle, Table 5 illustrates a corresponding 1 h rainfall intensity range of 44 to 50 mm/h. Consequently, 50 mm/h is designated as the benchmark for the 1 h rainfall intensity threshold  $x_{R2}$ , serving as a clear demarcation between moderate and high risk levels of waterlogging.

Table 5. List of the response relationships between 1 h rainfall intensity and waterlogging depth in Cluster 5.

Index	Cluster Category	Rainfall Intensity (mm/h)	Waterlogging Depth (m)	Index	Cluster Category	Rainfall Intensity (mm/h)	Waterlogging Depth (m)
1	Cluster 5	61	0.43	12	Cluster 5	45	0.40
2	Cluster 5	63	0.43	13	Cluster 5	50	0.40
3	Cluster 5	56	0.42	14	Cluster 5	47	0.39
4	Cluster 5	54	0.42	15	Cluster 5	43	0.38
5	Cluster 5	52	0.42	16	Cluster 5	63	0.38
6	Cluster 5	50	0.41	17	Cluster 5	48	0.37
7	Cluster 5	60	0.41	18	Cluster 5	58	0.37
8	Cluster 5	54	0.41	19	Cluster 5	44	0.36
9	Cluster 5	49	0.41	20	Cluster 5	52	0.36
10	Cluster 5	47	0.40	21	Cluster 5	49	0.35
11	Cluster 5	44	0.40				

In conclusion, the piecewise function for 1 h rainfall intensity water logging index  $f(x_R)$  is obtained, as shown in Equation (8):

$$f(x_R) = \begin{cases} 1, & x_R < 40 \\ 2, & 40 \leq x_R < 50 \\ 3, & x_R \geq 50 \end{cases} \quad (8)$$

### 3.2. Determination the Warning Levels for Building Waterlogging, Road Waterlogging, and Public Evacuation in Beijing’s Historic and Cultural Districts

According to the meteorological warning standards specified in the “Beijing waterlogging prevention control Emergency Plan (Revised in 2022),” when the meteorological department issues a blue warning, the expected rainfall intensity in the next 1 h will exceed 30 mm/h. A yellow warning signifies an expected rainfall intensity of more than 50 mm/h; an orange warning indicates an expected intensity exceeding 70 mm/h, and a red warning suggests an intensity exceeding 100 mm/h. Based on the principle of determining the 1 h rainfall intensity water logging index  $f(x_R)$  for a specific historical and cultural district

in Beijing according to formula (8), the specific values for the 1 h rainfall intensity water logging index in the third column of Table 6 can be derived. By multiplying these values with the risk indices for building waterlogging, road waterlogging, and public evacuation, it is possible to accurately assess the warning levels faced by buildings, roads, and the public in the district. It is essential to classify these indicators separately as buildings, roads, and public evacuation exhibit distinct resilience characteristics during the early-warning process. The importance of this classification lies in highlighting the disparities among the three, emphasizing their unique attributes and responses to potential risks. In Table 6, blue represents low risk, yellow represents moderate risk, orange indicates relatively high risk, and red signifies high risk.

**Table 6.** The correspondence between the warning level and the meteorological rainstorm warning level, the 1 h rainfall intensity water logging index, and the waterlogging risk index in historical and cultural districts.

Meteorological Rainstorm Warning Level	Rainfall Intensity in the Next 1 h (mm/h)	1 h Rainfall Intensity Water Logging Index	Building Water Logging Risk Index	Building Water Logging Warning Levels	Road Water Logging Risk Index	Building Water Logging Warning Levels	Public Evacuation Index	Public Evacuation Warning Levels
Blue Alert	30	1	1	Blue	1	Blue	1	Blue
			2	Yellow	2	Yellow	2	Yellow
			3	Orange	3	Orange	3	Orange
Yellow Alert	50	2	1	Yellow	1	Yellow	1	Yellow
			2	Orange	2	Orange	2	Orange
			3	Red	3	Red	3	Red
Orange Alert	70	3	1	Orange	1	Orange	1	Orange
			2	Red	2	Red	2	Red
			3	Red	3	Red	3	Red
Red Alert	100	3	1	Orange	1	Orange	1	Orange
			2	Red	2	Red	2	Red
			3	Red	3	Red	3	Red

*3.3. Development of Early-Warning Response Measures for Building Waterlogging, Road Waterlogging, and Public Evacuation in Beijing’s Historic and Cultural Districts*

When a heavy rainstorm approaches, the waterlogging prevention control headquarters of the historic and cultural districts should issue warning information. The emergency response work for rainstorm-induced waterlogging should follow the procedures outlined in Table 7. With changes in the hourly rainfall intensity forecast by the meteorological department, the warning level should be dynamically adjusted and updated information should be issued. The responding entities should dynamically adjust their warning response measures. These response measures should include both technical and non-technical aspects that complement each other. The emergency response entities should immediately activate the response measures according to their respective responsibilities. The following response measures should be included in the emergency waterlogging prevention plan and adjusted and revised in time according to various changes in the pre-waterlogging warning targets, response measures, and responding entities. The issuance, modification, and lifting of warnings for building waterlogging, road waterlogging, and public evacuation in the district should be highly consistent with the heavy rain warning information issued by the municipal meteorological department and the district-level flood warning.

**Table 7.** Early-warning response measures for building waterlogging, road waterlogging, and public evacuation in the district.

Alert Objects in the District	Warning Levels	Risk Characteristics	Response Measures		Response Entities
			Technical	Nontechnical	
District’s buildings	Blue Alert	Potential water ingress	Prepare flood barriers and sandbags	Inspection and investigation; Information submission	
District’s roads		Potential water accumulation	Water pumping operation; Clear blockage at rainwater outlets	Inspection and investigation; Information submission	
District’s residents		Pose risks to occupants of dangerous buildings	Evacuation and relocation of occupants in dangerous buildings and elderly people living alone	Inspection and investigation; Information submission	
District’s buildings	Yellow Alert	High risk of water ingress; Potential roof leaks	Install flood barriers, sandbags, and drainage pumps; Use tarpaulin or roofing felt to cover and repair leaking roofs	Inspection and investigation; Information submission; Emergency repair scheduling	Waterlogging prevention control headquarters of the street where the historic and cultural district is located; Waterlogging prevention control headquarters of cultural heritage units; Various emergency rescue teams; The public in historical and cultural districts
District’s roads		High risk of water accumulation	Clear away the accumulated water; Install drainage units;	Inspection and investigation; Information submission; Forced drainage scheduling	
District’s residents		Threat to elderly and children	Organize the evacuation of elderly and children as needed	Household survey; Shelter preparation; Information submission	
District’s buildings	Orange Alert	High risk of water ingress; Potential roof leaks	Start the operation of drainage pumps as needed; Use tarpaulin or roofing felt to cover and repair leaking roofs	Inspection and investigation; Information submission; Emergency repair scheduling	
District’s roads		High risk of water accumulation	Start the operation of drainage pumps as needed	Inspection and investigation; Information submission; Road closure control; Personnel and vehicle detour; Notify to move vehicles	
District’s residents		Significant threat to elderly and children	Organize the evacuation of elderly and children as needed; Evacuate personnel from schools, scenic areas, and organizations within the neighborhood	Inspection and investigation; Information submission; Organize evacuation	

Table 7. Cont.

Alert Objects in the District	Warning Levels	Risk Characteristics	Response Measures		Response Entities
			Technical	Nontechnical	
District’s buildings	Red Alert	Water ingress occurs; Extensive roof leaks occur	Start the operation of drainage pumps as needed; Use tarpaulin or roofing felt to cover and repair leaking roofs	Inspection and investigation; Information submission; Emergency repair scheduling	Waterlogging prevention control headquarters of the street where the historic and cultural district is located;
District’s roads		Water accumulation occurs; Road surface collapse occurs	Start the operation of drainage units; Road repair and barricading	Inspection and investigation; Information submission; Road closure control; Personnel and vehicle detour	Waterlogging prevention control headquarters of cultural heritage units;
District’s residents		Poses a threat to the majority of the public	Public prepares for evacuation; Organize public evacuation as needed; Emergency medical rescue	Inspection and investigation; Information submission; Organize evacuation	Various emergency rescue teams; The public in historical and cultural districts

This paper adopts a comprehensive approach that integrates mathematical modeling, model simulations, and resilience assessments to establish a refined waterlogging warning system tailored for a historic and cultural district in Beijing, China, under rainstorm scenarios. When crafting the refined rainstorm-induced waterlogging early-warning model, this study fully considers the limitations of monitoring data, particularly for rainstorm events that occur once a century or are rarer. Due to their extremely low occurrence frequency, corresponding historical monitoring data are severely insufficient. Therefore, we adopt the method of model simulation to compensate for data deficiencies by simulating the interaction between rainfall intensity and water accumulation depth. The simulation methodology for rainstorm-induced waterlogging models is well established and widely employed in the academic community, providing strong support for this article [45–47]. Building upon previous research, this paper further expands the analytical approach for simulation results by applying cluster analysis to reveal the relationship between rainfall intensity and water accumulation depth. Additionally, flood resilience assessment is introduced as an important component of the warning model construction. Flood resilience assessment can more accurately reflect the resistance, absorption, adaptation, and recovery capabilities of disaster-bearing bodies during rainstorm events [48–50], exhibiting stronger objectivity compared to traditional risk level assessment methods for rainstorm waterlogging. Through resilience assessments, it becomes possible to derive the waterlogging risk index more accurately, providing a more scientific and reasonable decision-making basis for waterlogging warnings and pre-disaster emergency responses in historical and cultural districts.

Through a rigorous analysis and determination of the 1 h rainfall intensity water logging index within a historic and cultural district in Beijing, this study establishes critical thresholds for meteorological forecasts. Specifically, the thresholds for low and medium risks of future 1 h rainfall are set at 40 mm/h, whereas the thresholds for medium and high risks are designated as 50 mm/h. Upon comparing these thresholds with available data, it becomes evident that they closely correlate with the meteorological characteristics of Beijing’s urban landscapes and the current drainage capabilities of its historic and cultural districts [51,52]. Furthermore, these thresholds align seamlessly with the prevailing meteorological warning standards in Beijing, thus underscoring the scientific validity of the determination method employed in this study for the 1 h rainfall intensity water logging index.

Compared to the traditional monitoring-based waterlogging early-warning models, the refined early-warning model introduced in this article offers distinct advantages in terms of pre-disaster positioning and control [53,54]. Within the confines of meteorological forecast timeframes, this model can accurately assess the warning levels for buildings, roads, and the general public within the historic and cultural district. Depending on the severity levels indicated by the red, orange, yellow, and blue warnings, appropriate emergency response measures can be promptly implemented, including evacuating residents, closing roads, activating drainage facilities, and so on (detailed in Table 7). This approach helps to enhance the accuracy and timeliness of waterlogging warnings, thereby reducing the impact of waterlogging disasters on the historic and cultural district.

Furthermore, this model possesses high flexibility and scalability, allowing for adjustments and optimizations based on actual conditions to cater to the waterlogging warning needs of various historic and cultural districts under different rainfall conditions.

#### 4. Conclusions

This article proposes a method for constructing a refined early-warning model for rainstorm-induced waterlogging in Beijing's historic and cultural districts. By establishing the mathematical relationships between 1 h rainfall intensity water logging index and the building waterlogging risk index, road waterlogging risk index, and public evacuation index, we derive a building waterlogging early-warning model  $f(W_{BD})$ , a road waterlogging early-warning model  $f(W_{RD})$ , and a public evacuation early-warning model  $f(W_{OC})$ .

This paper thoroughly discusses the determination method of the piecewise function  $f(x_R)$  for the 1 h rainfall intensity water logging index. The 1 h rainfall intensity water logging index serves as the pivotal indicator for establishing the response relationship between meteorological forecast warnings and the characteristics of waterlogging in the district. In terms of method integration, the simulation method of the hydrological and hydrodynamic model of the district is coupled with cluster analysis to objectively reveal the dynamic relationship between the designed rainfall intensity and waterlogging in the district. In the numerical analysis, 0.27 m and 0.4 m are chosen as two critical thresholds for determining the risk of waterlogging, which are used to derive the designed rainfall intensity corresponding to the critical thresholds, thus obtaining a piecewise function  $f(x_R)$  that meets the characteristics of waterlogging risk in Beijing's historic and cultural districts.

Based on the evaluation of flood resilience in buildings, roads, and society within the historic and cultural districts, the determination method of the waterlogging risk index for the district is discussed. The flood resilience of buildings, roads, and society within the district can directly reflect the correlation between characteristic parameters such as depth, flow velocity, and the risk of functional loss after waterlogging. Therefore, this study proposes a method for deriving the segmentation functions of the building waterlogging risk index  $f(Res_{BD})$ , road waterlogging risk index  $f(Res_{RD})$ , and public evacuation index  $f(Res_{OC})$  based on resilience level assessments. This method can more accurately describe the dynamic process of waterlogging risks varying with rainfall intensity and better align with the actual situation of waterlogging risks in the district.

Empirical validation was conducted on the refined early-warning model for rainstorm-induced waterlogging in Beijing's historic and cultural districts proposed in this paper, using actual cases from these districts. By determining 1 h rainfall intensity water logging index for the districts, clarifying warning levels, and formulating scientifically reasonable warning response measures, the practical application value of this model in emergency waterlogging prevention control and rescue work in Beijing's historic and cultural districts was elucidated. Assessing and dynamically adjusting the warning levels and response measures for buildings, roads, and the public in the district are crucial, as they will contribute to improving the efficiency and accuracy of rescue operations within the precious forecast time.

Future research should further focus on the applicability of the refined early-warning model in different flood disasters, not just rainstorm-induced waterlogging, deeply analyz-

ing its warning function throughout the entire lifecycle of flood prevention and emergency management. Additionally, it is necessary to strengthen and explore the linkage mechanism between rainstorm waterlogging monitoring and early warning, ensuring close coordination between the two. By fully utilizing daily monitoring data and historical disaster information, objective evidence can be provided for validating and optimizing the refined early-warning model for rainstorm-induced waterlogging. Moreover, attention should be given to the continuous optimization and improvement of warning response measures to ensure the precision and efficiency of warning management strategies. The amount of early-warning time that can be saved through these efforts remains a question worthy of deep reflection, as it involves not only issues with early-warning methods but also numerous management considerations. This article only explores the subject from the perspective of methods to improve the accuracy and timeliness of early warnings, without conducting a comprehensive social survey on the emergency management capabilities of historic and cultural districts. Therefore, quantifying and evaluating the early-warning issuance time for different historic and cultural districts remains a topic worthy of continuous and in-depth research. In summary, sustained and profound exploration in this field is of great significance for ensuring the sustainable development of historic cities and historic and cultural districts.

**Author Contributions:** Conceptualization, J.W. and J.L. (Junqi Li); methodology, J.W. and J.L. (Junqi Li); software, J.W., Y.L. and Y.Z.; validation, J.W., L.X., J.L. (Jing Li) and X.W.; data curation, J.W.; writing—original draft preparation, J.W. and J.L. (Junqi Li); writing—review and editing, J.W., T.X. and J.L. (Junqi Li); supervision, L.X., J.L. (Jing Li) and X.W. All authors have read and agreed to the published version of the manuscript.

**Funding:** This work was supported by National Natural Science Foundation of China (52370093).

**Data Availability Statement:** The data presented in this study are available on request from the corresponding author.

**Conflicts of Interest:** The authors declare no conflicts of interest.

## References

1. D’Ayala, D.; Wang, K.; Yan, Y.; Smith, H.; Massam, A.; Filipova, V.; Pereira, J.J. Flood Vulnerability and Risk Assessment of Urban Traditional Buildings in a Heritage District of Kuala Lumpur, Malaysia. *Nat. Hazards Earth Syst. Sci.* **2020**, *20*, 2221–2241. [[CrossRef](#)]
2. Aribisala, O.D.; Yum, S.-G.; Adhikari, M.D.; Song, M.-S. Flood Damage Assessment: A Review of Microscale Methodologies for Residential Buildings. *Sustainability* **2022**, *14*, 13817. [[CrossRef](#)]
3. Arrighi, C.; Rossi, L.; Trasforini, E.; Rudari, R.; Ferraris, L.; Brugioni, M.; Franceschini, S.; Castelli, F. Quantification of Flood Risk Mitigation Benefits: A Building-Scale Damage Assessment through the RASOR Platform. *J. Environ. Manag.* **2018**, *207*, 92–104. [[CrossRef](#)] [[PubMed](#)]
4. Pandey, A.C.; Singh, S.K.; Nathawat, M.S. Waterlogging and Flood Hazards Vulnerability and Risk Assessment in Indo Gangetic Plain. *Nat. Hazards* **2010**, *55*, 273–289. [[CrossRef](#)]
5. Subrina, S.; Chowdhury, F.K. Urban Dynamics: An Undervalued Issue for Water Logging Disaster Risk Management in Case of Dhaka City, Bangladesh. *Procedia Eng.* **2018**, *212*, 801–808. [[CrossRef](#)]
6. Samuels, K.L.; Platts, E.J. Global Climate Change and UNESCO World Heritage. *Int. J. Cult. Prop.* **2022**, *29*, 409–432. [[CrossRef](#)]
7. Kundzewicz, Z.W. Non-Structural Flood Protection and Sustainability. *Water Int.* **2002**, *27*, 3–13. [[CrossRef](#)]
8. Egusquiza, A.; Lückerrath, D.; Zorita, S.; Silvertown, S.; Garcia, G.; Servera, E.; Bonazza, A.; Garcia, I.; Kalis, A. Paving the Way for Climate Neutral and Resilient Historic Districts. *Open Res. Eur.* **2023**, *3*, 42. [[CrossRef](#)]
9. Sesana, E.; Gagnon, A.S.; Ciantelli, C.; Cassar, J.; Hughes, J.J. Climate Change Impacts on Cultural Heritage: A Literature Review. *WIREs Clim. Chang.* **2021**, *12*, e710. [[CrossRef](#)]
10. Lu, J.; Li, F.; Wang, Y. Experience and Enlightenment of Urban Waterlogging Disaster Prevention in Foreign Countries. *E3S Web Conf.* **2022**, *352*, 03010. [[CrossRef](#)]
11. Alfieri, L.; Salamon, P.; Pappenberger, F.; Wetterhall, F.; Thielen, J. Operational Early Warning Systems for Water-Related Hazards in Europe. *Environ. Sci. Policy* **2012**, *21*, 35–49. [[CrossRef](#)]
12. Cerra, D.; Plank, S. Towards Early Warning for Damages to Cultural Heritage Sites: The Case of Palmyra. In *Remote Sensing for Archaeology and Cultural Landscapes: Best Practices and Perspectives Across Europe and the Middle East*; Hadjimitsis, D.G., Themistocleous, K., Cuca, B., Agapiou, A., Lysandrou, V., Lasaponara, R., Masini, N., Schreier, G., Eds.; Springer International Publishing: Cham, Switzerland, 2020; pp. 221–239. ISBN 978-3-030-10979-0.

13. Kittipongvises, S.; Phetrak, A.; Rattanapun, P.; Brundiens, K.; Buizer, J.L.; Melnick, R. AHP-GIS Analysis for Flood Hazard Assessment of the Communities Nearby the World Heritage Site on Ayutthaya Island, Thailand. *Int. J. Disaster Risk Reduct.* **2020**, *48*, 101612. [[CrossRef](#)]
14. Acosta-Coll, M.; Ballester-Merelo, F.; Martinez-Peiró, M.; De la Hoz-Franco, E. Real-Time Early Warning System Design for Pluvial Flash Floods—A Review. *Sensors* **2018**, *18*, 2255. [[CrossRef](#)] [[PubMed](#)]
15. Wei, M.; She, L.; You, X. Establishment of Urban Waterlogging Pre-Warning System Based on Coupling RBF-NARX Neural Networks. *Water Sci. Technol.* **2020**, *82*, 1921–1931. [[CrossRef](#)] [[PubMed](#)]
16. Liu, J.; Mei, C.; Liu, H.; Fang, X.; Ni, G.; Jin, W. Key Scientific and Technological Issues of Joint Prevention and Control of River Flood and Urban Waterlogging Disaster Chain in Megacities. *Adv. Water Sci.* **2023**, *34*, 172–181. [[CrossRef](#)]
17. Liu, Y.; Liu, W.; Lin, Y.; Zhang, X.; Zhou, J.; Wei, B.; Nie, G.; Gross, L. Urban Waterlogging Resilience Assessment and Postdisaster Recovery Monitoring Using NPP-VIIRS Nighttime Light Data: A Case Study of the 'July 20, 2021' Heavy Rainstorm in Zhengzhou City, China. *Int. J. Disaster Risk Reduct.* **2023**, *90*, 103649. [[CrossRef](#)]
18. Lin, J.; He, P.; Yang, L.; He, X.; Lu, S.; Liu, D. Predicting Future Urban Waterlogging-Prone Areas by Coupling the Maximum Entropy and FLUS Model. *Sustain. Cities Soc.* **2022**, *80*, 103812. [[CrossRef](#)]
19. Hou, J.; Du, Y. Spatial Simulation of Rainstorm Waterlogging Based on a Water Accumulation Diffusion Algorithm. *Geomat. Nat. Hazards Risk* **2020**, *11*, 71–87. [[CrossRef](#)]
20. Segoni, S.; Battistini, A.; Rossi, G.; Rosi, A.; Lagomarsino, D.; Catani, F.; Moretti, S.; Casagli, N. Technical Note: An Operational Landslide Early Warning System at Regional Scale Based on Space–Time-Variable Rainfall Thresholds. *Nat. Hazards Earth Syst. Sci.* **2015**, *15*, 853–861. [[CrossRef](#)]
21. Alfieri, L.; Zsoter, E.; Harrigan, S.; Aga Hirpa, F.; Lavaysse, C.; Prudhomme, C.; Salamon, P. Range-Dependent Thresholds for Global Flood Early Warning. *J. Hydrol. X* **2019**, *4*, 100034. [[CrossRef](#)] [[PubMed](#)]
22. Cools, J.; Innocenti, D.; O'Brien, S. Lessons from Flood Early Warning Systems. *Environ. Sci. Policy* **2016**, *58*, 117–122. [[CrossRef](#)]
23. Roy, S.; Bose, A.; Singha, N.; Basak, D.; Chowdhury, I.R. Urban Waterlogging Risk as an Undervalued Environmental Challenge: An Integrated MCDA-GIS Based Modeling Approach. *Environ. Chall.* **2021**, *4*, 100194. [[CrossRef](#)]
24. Subashini, M.J.; Sudarmani, R.; Gobika, S.; Varshini, R. Development of Smart Flood Monitoring and Early Warning System Using Weather Forecasting Data and Wireless Sensor Networks-A Review. In Proceedings of the 2021 Third International Conference on Intelligent Communication Technologies and Virtual Mobile Networks (ICICV), Tirunelveli, India, 4–6 February 2021; pp. 132–135.
25. Sun, R.; Shi, S.; Rehemani, Y.; Li, S. Measurement of Urban Flood Resilience Using a Quantitative Model Based on the Correlation of Vulnerability and Resilience. *Int. J. Disaster Risk Reduct.* **2022**, *82*, 103344. [[CrossRef](#)]
26. Bulti, D.T.; Girma, B.; Megento, T.L. Community Flood Resilience Assessment Frameworks: A Review. *SN Appl. Sci.* **2019**, *1*, 1663. [[CrossRef](#)]
27. Cheng, Y.; Elsayed, E.A.; Huang, Z. Systems Resilience Assessments: A Review, Framework and Metrics. *Int. J. Prod. Res.* **2022**, *60*, 595–622. [[CrossRef](#)]
28. Golz, S.; Schinke, R.; Naumann, T. Assessing the Effects of Flood Resilience Technologies on Building Scale. *Urban Water J.* **2015**, *12*, 30–43. [[CrossRef](#)]
29. Keating, A.; Campbell, K.; Szoenyi, M.; McQuistan, C.; Nash, D.; Burer, M. Development and Testing of a Community Flood Resilience Measurement Tool. *Nat. Hazards Earth Syst. Sci.* **2017**, *17*, 77–101. [[CrossRef](#)]
30. Irwin, S.; Schardong, A.; Simonovic, S.P.; Nirupama, N. ResilSIM—A Decision Support Tool for Estimating Resilience of Urban Systems. *Water* **2016**, *8*, 377. [[CrossRef](#)]
31. Chen, Z.; Li, K.; Du, J.; Chen, Y.; Liu, R.; Wang, Y. Three-Dimensional Simulation of Regional Urban Waterlogging Based on High-Precision DEM Model. *Nat. Hazards* **2021**, *108*, 2653–2677. [[CrossRef](#)]
32. Chowdhury, M.S. Modelling Hydrological Factors from DEM Using GIS. *MethodsX* **2023**, *10*, 102062. [[CrossRef](#)] [[PubMed](#)]
33. Cimellaro, G.P.; Renschler, C.; Reinhorn, A.M.; Arendt, L. PEOPLES: A Framework for Evaluating Resilience. *J. Struct. Eng.* **2016**, *142*, 04016063. [[CrossRef](#)]
34. Dewulf, A.; Karpouzoglou, T.; Warner, J.; Wesselink, A.; Mao, F.; Vos, J.; Tamas, P.; Groot, A.E.; Heijmans, A.; Ahmed, F.; et al. The Power to Define Resilience in Social-Hydrological Systems: Toward a Power-Sensitive Resilience Framework. *WIREs Water* **2019**, *6*, e1377. [[CrossRef](#)]
35. Graveline, M.-H.; Germain, D. Disaster Risk Resilience: Conceptual Evolution, Key Issues, and Opportunities. *Int. J. Disaster Risk Sci.* **2022**, *13*, 330–341. [[CrossRef](#)]
36. Meerow, S.; Newell, J.P.; Stults, M. Defining Urban Resilience: A Review. *Landsc. Urban Plan.* **2016**, *147*, 38–49. [[CrossRef](#)]
37. Zhao, L.; He, F.; Zhao, C. A Framework of Resilience Development for Poor Villages after the Wenchuan Earthquake Based on the Principle of "Build Back Better". *Sustainability* **2020**, *12*, 4979. [[CrossRef](#)]
38. Chen, W.; Huang, G.; Zhang, H. Urban Stormwater Inundation Simulation Based on SWMM and Diffusive Overland-Flow Model. *Water Sci. Technol.* **2017**, *76*, 3392–3403. [[CrossRef](#)] [[PubMed](#)]
39. Sidek, L.M.; Jaafar, A.S.; Majid, W.H.A.W.A.; Basri, H.; Marufuzzaman, M.; Fared, M.M.; Moon, W.C. High-Resolution Hydrological-Hydraulic Modeling of Urban Floods Using InfoWorks ICM. *Sustainability* **2021**, *13*, 10259. [[CrossRef](#)]
40. Zhang, Z.; Liu, D.; Zhang, R.; Li, J.; Wang, W. The Impact of Rainfall Change on Rainwater Source Control in Beijing. *Urban Clim.* **2021**, *37*, 100841. [[CrossRef](#)]

41. Creaco, E. Scaling Models of Intensity–Duration–Frequency (IDF) Curves Based on Adjusted Design Event Durations. *J. Hydrol.* **2024**, *632*, 130847. [[CrossRef](#)]
42. Mottahedin, A.; Giudicianni, C.; Barbero, G.; Petaccia, G.; Creaco, E. General Method Based on Regressive Relationships to Parameterize the Three-Parameter Depth-Duration-Frequency Curve. *Atmosphere* **2023**, *14*, 190. [[CrossRef](#)]
43. Ahmed, M.; Seraj, R.; Islam, S.M.S. The K-Means Algorithm: A Comprehensive Survey and Performance Evaluation. *Electronics* **2020**, *9*, 1295. [[CrossRef](#)]
44. Xu, H.; Ma, C.; Lian, J.; Xu, K.; Chaima, E. Urban Flooding Risk Assessment Based on an Integrated K-Means Cluster Algorithm and Improved Entropy Weight Method in the Region of Haikou, China. *J. Hydrol.* **2018**, *563*, 975–986. [[CrossRef](#)]
45. Cheng, T.; Xu, Z.; Hong, S.; Song, S. Flood Risk Zoning by Using 2D Hydrodynamic Modeling: A Case Study in Jinan City. *Math. Probl. Eng.* **2017**, *2017*, e5659197. [[CrossRef](#)]
46. Fan, Y.; Ao, T.; Yu, H.; Huang, G.; Li, X. A Coupled 1D-2D Hydrodynamic Model for Urban Flood Inundation. *Adv. Meteorol.* **2017**, *2017*, e2819308. [[CrossRef](#)]
47. Teng, J.; Jakeman, A.J.; Vaze, J.; Croke, B.F.W.; Dutta, D.; Kim, S. Flood Inundation Modelling: A Review of Methods, Recent Advances and Uncertainty Analysis. *Environ. Model. Softw.* **2017**, *90*, 201–216. [[CrossRef](#)]
48. Parsons, M.; Glavac, S.; Hastings, P.; Marshall, G.; McGregor, J.; McNeill, J.; Morley, P.; Reeve, I.; Stayner, R. Top-down Assessment of Disaster Resilience: A Conceptual Framework Using Coping and Adaptive Capacities. *Int. J. Disaster Risk Reduct.* **2016**, *19*, 1–11. [[CrossRef](#)]
49. McClymont, K.; Morrison, D.; Beevers, L.; Carmen, E. Flood Resilience: A Systematic Review. *J. Environ. Plan. Manag.* **2020**, *63*, 1151–1176. [[CrossRef](#)]
50. Ostadtaghizadeh, A.; Ardalan, A.; Paton, D.; Jabbari, H.; Khankeh, H.R. Community Disaster Resilience: A Systematic Review on Assessment Models and Tools. *PLoS Curr.* **2015**, *7*, ecurrents.dis.f224ef8efbdfcf1d508dd0de4d8210ed. [[CrossRef](#)] [[PubMed](#)]
51. Shin, H.B. Urban Conservation and Revalorisation of Dilapidated Historic Quarters: The Case of Nanluoguxiang in Beijing. *Cities* **2010**, *27*, S43–S54. [[CrossRef](#)]
52. Cun, C.; Zhang, W.; Che, W.; Sun, H. Review of Urban Drainage and Stormwater Management in Ancient China. *Landsc. Urban Plan.* **2019**, *190*, 103600. [[CrossRef](#)]
53. Ding, J.; Cai, J.; Guo, G.; Chen, C. An Emergency Decision-Making Method for Urban Rainstorm Water-Logging: A China Study. *Sustainability* **2018**, *10*, 3453. [[CrossRef](#)]
54. Ding, Y.; Wang, H.; Liu, Y.; Lei, X. Urban Waterlogging Structure Risk Assessment and Enhancement. *J. Environ. Manag.* **2024**, *352*, 120074. [[CrossRef](#)] [[PubMed](#)]

**Disclaimer/Publisher’s Note:** The statements, opinions and data contained in all publications are solely those of the individual author(s) and contributor(s) and not of MDPI and/or the editor(s). MDPI and/or the editor(s) disclaim responsibility for any injury to people or property resulting from any ideas, methods, instructions or products referred to in the content.